Earthquake Engineering, Tenth World Conference © 1992 Balkema, Rotterdam. ISBN 90 5410 060 5

A study on the characteristics of seismic vertical motion

N. Fujii, T. Annaka & H. Ohki
Tokyo Electric Power Services Co., Ltd, Japan

M. Fujitani & N. Yasuda
Tokyo Electric Power Co., Ltd, Japan

ABSTRACT: It was indicated that P wave propagation theory can be applied to the vertical response analysis of soil. For examining the relationships between vertical and horizontal motions, a simulation method for obtaining both vertical and horizontal synthetic accelerograms was proposed. Using the mean relationships of the simulation parameters at the design base layer, it is possible to simulate a vertical motion from a given horizontal motion.

1 INTRODUCTION

For the precise evaluation of seismic soil response, both horizontal and vertical motions should be considered in the analysis. However, it has not become clear that P wave propagation theory can be applied to the evaluation of vertical soil response. Furthermore, no practical method for deriving a vertical input motion from a horizontal input motion defined at a design base layer is established. The S wave velocity of the design base layer in the metropolitan area of the Kanto district, Japan, is usually greater than or equal to 300 m/s. The purposes of the present study are to examine the applicability of P wave propagation theory to the vertical soil response analysis and to propose a practical method for deriving a vertical motion from a horizontal motion given at the design base layer.

2 SOIL RESPONSE TO VERTICAL MOTION

The time history of a vertical ground motion generally has two peaks. The first peak appears in a P wave portion following the arrival of P wave. The P wave portion is mainly related to direct P wave from a seismic source, therefore the soil response of the P wave portion can ideally be modelled by 1-D P wave propagation theory. The second peak appears in a S wave portion following the arrival of S wave. The S wave portion is mainly related to direct S wave from the seismic source. The horizontal soil response of the S wave portion, accordingly, can ideally be modelled by 1-D S wave propagation theory. The vertical motion of the S wave portion may be caused by converted P waves generated from direct S wave at some discontinuity near a site or by obliquely incident SV waves. The applicability of 1-D P wave propagation theory to the vertical motion of the S wave portion is not clear. The P and S wave portions, therefore, were separately analyzed.

Strong ground motion accelerograms obtained by seismic vertical arrays developed in the Kanto district were analyzed. Figure 1 shows the distribution of the observation sites. The seismic vertical arrays are installed at the sites from A to F. The data at M will be used in the following section. Locations of vertical-motion seismometers and P and S wave velocity structures used in the analysis for each seismic vertical array are shown in Fig.2. The velocity structures at A, B, and D, were determined by in situ seismic velocity measurements. Although the soil profiles by boring logs have been obtained for the other three sites, C, E and F, in situ seismic velocity measurements have not been performed. The velocity structures shown in Fig.2 were obtained by modifying, if necessary, the initial models derived from in situ measurements to make the theoretical spectral ratios between ground surface and underground motions match those obtained by the corresponding recorded motions. The P wave velocity structure of the site D was not modified, whereas those of the sites A and B were slightly changed. The details will be explained below.

The spectral ratios of recorded vertical accelerograms between ground surface and underground were compared with those calculated theoretically from the soil models by 1-D P wave propagation theory as shown in Fig.3.

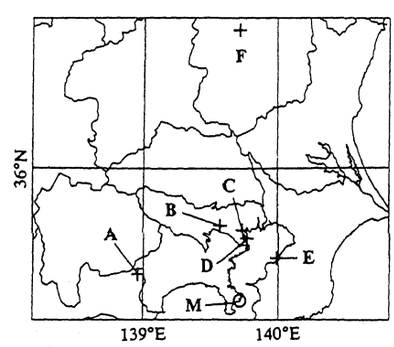

Fig.1 Distribution of observation sites.

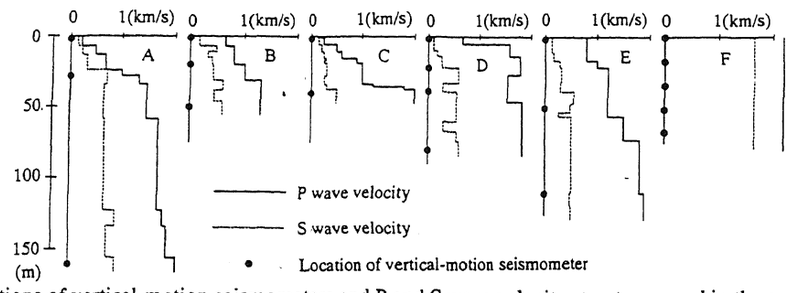

Fig.2 Locations of vertical-motion seismometers and P and S wave velocity structures used in the analysis for each seismic vertical array.

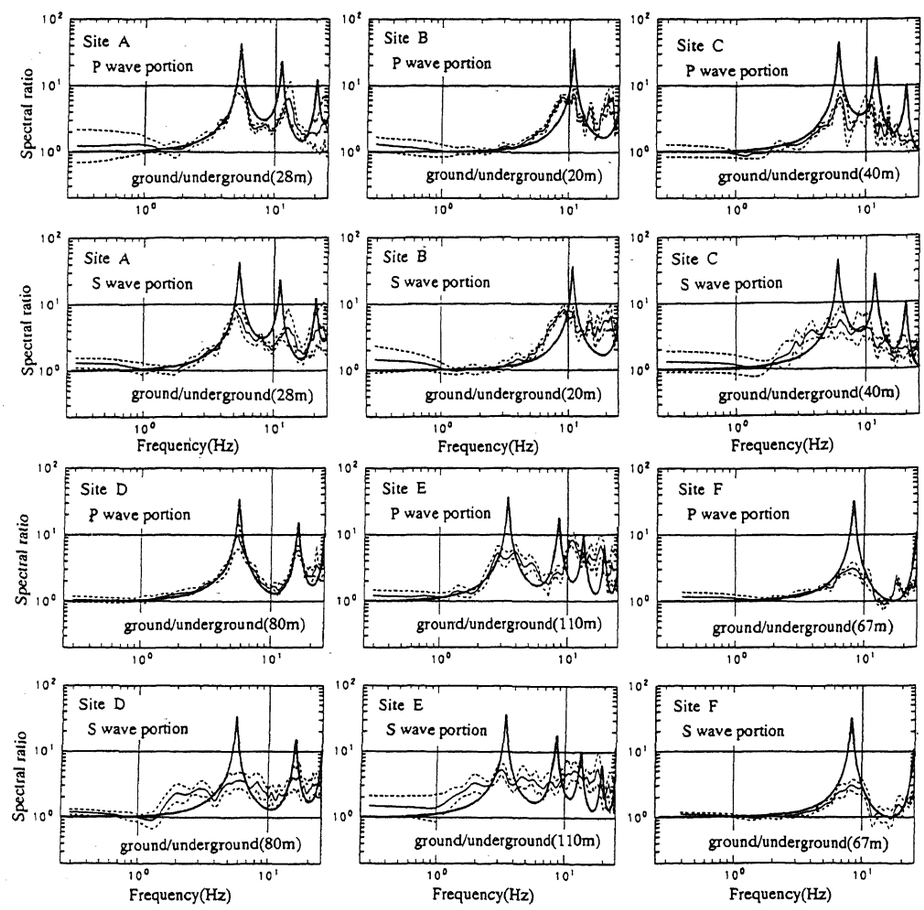

Fig.3 Comparison between the spectral ratios of the recorded vertical motions and those calculated theoretically from the soil models. The details are explained in the text.

The spectral ratios of the recorded motions were separately calculated for the P and S wave portions. Thin solid line denotes the mean of the spectral ratios obtained by the recorded motions and two broken lines denote the mean ± one standard deviation. We used the records of seven earthquakes from 1985 through 1987 at A, four earthquakes from 1986 through 1987 at B, five earthquakes from 1985 through 1986 at C, thirteen earthquakes from 1982 through 1986 at D, eight earthquakes from 1984 through 1985 at E, and three earthquakes from 1987 through 1988 at F. Smooth thick solid line denotes the theoretically calculated spectral

ratio from the soil models shown in Fig.2 by 1-D P wave propagation theory. The damping ratio of the soil was assumed as 2 %.

For P wave portion, predominant peaks are clearly seen in the spectral ratios of the recorded motions for all six sites. Each soil model used in the calculation was determined so that the first predominant frequency of the spectral ratios calculated by 1-D P wave propagation theory can agree with that obtained from the P wave portion of the recorded motions. The agreement of the spectral ratios between the recorded motions and the theory is very well for the site D whose velocity structure is directly determined by in situ measurement. It appears that the spectral ratios of the recorded motions for the P wave portion can be explained by 1-D P wave propagation theory because the assumption of vertical incident P wave is almost fully satisfied .

On the other hand the spectral ratios of the recorded motions for the S wave portion can be grouped into two types. The first type is that the predominant peaks exist at the same frequencies as the P wave portion. The spectral ratios of the recorded motions at A, B and F are classified into this type. In these sites the spectral ratios of the recorded motions can be explained by 1-D P wave propagation theory similarly to the P wave portion. The second type is that the predominant peaks are not so clear as the P wave portion. However, the small peaks in the the spectral ratios of the recorded motions can be seen around the peak frequencies of the theoretical ratios. The spectral ratios of the recorded motions at C, D and E are classified into this type.

For estimating the interval propagation velocities of vertical motions at C, D and E, time-lags between surface and underground motions which maximize the cross-correlation coefficients between the two motions were determined. Figure 4 shows the relation between time-lag and cross-correlation coefficient for the site D. The coefficients are plotted at depths where the used underground motions were obtained. Two peaks of cross-correlation coefficients, which are related to upward and downward propagating waves respectively, can be seen commonly for both the P and S wave portions at the depth of about 80 m. The time-lags of the peaks for the P and S wave portions are 0.05 sec and 0.04 sec respectively. The expected lag-time by the P wave velocity structure is 0.048 sec, while that by the S wave velocity structure is 0.27 sec. The vertical motions of both the P and S wave portions, therefore, probably propagate with P wave velocity. For the sites C and E, the time-lags for the S wave portion could not be clearly determined: however, the cross-correlation coefficients between surface and underground motions were found to be maximum around the lag-time of 0.0 sec. This is not inconsistent with the assumption of P wave propagation.

The underground motions were calculated by 1-D P wave propagation theory using the observed ground surface motion as the input. The calculated vertical distributions of peak accelerations for the S wave portion are compared with those observed as shown in Fig.5. The agreement between the observations and the calculations is fairly good. The comparison between observed and calculated waveforms is shown in Fig.6. The waveforms

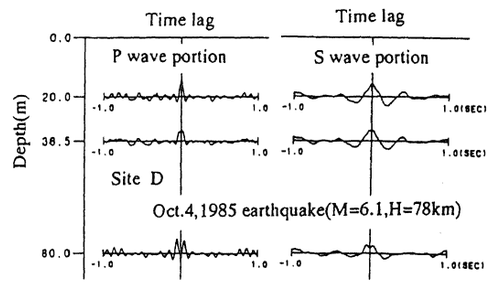

Fig.4 Relation between time-lag and cross-correlation coefficient.

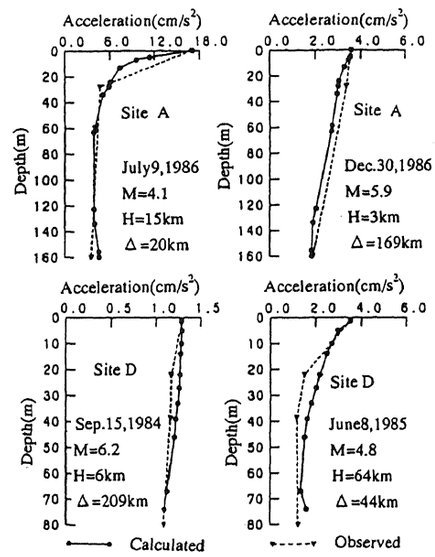

Fig.5 Comparison between the observed and calculated vertical distributions of peak accelerations.

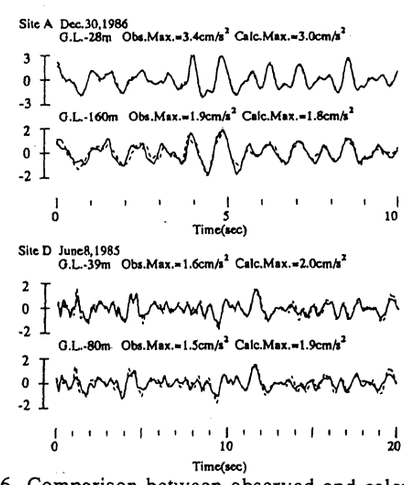

Fig.6 Comparison between observed and calculated waveforms: Solid line observed, Broken line calculated.

also agree very well.

The above results show that the main characteristics of seismic vertical response of soil can be simulated by 1-D P wave propagation theory. The S wave portion of vertical motion as well as the P wave portion is consistent with P wave propagation theory. Further investigation is naturally needed to make clear the cause for the difference of the two types in the spectral ratios of the recorded motions for the S wave portion and the wave conversion process from S to P. The lack of predominant peaks in the spectral ratios for the S wave portion can be attributed to the fact that the wave component of vertical motion of the S wave portion is not purely constructed by P wave: SV or surface waves may be included.

3 RELATIONSHIPS BETWEEN VERTICAL AND HORIZONTAL MOTIONS

In order to investigate the relationships between vertical and horizontal motions more precisely, a simulation method for obtaining synthetic horizontal accelerograms proposed by Izutani(1981) was extended to be applicable also to vertical motions. Izutani(1981) used the cumulative power curves of narrow band-pass filtered accelerograms. As shown in Fig.7, the cumulative power curve is modeled by three parameters: total power(E_i), starting time(t_i) and duration(D_i). The normalized cumulative power curve, $P_i(t)$, is obtained by dividing the cumulative power curve by the total power E_i. The starting time, t_i, is defined as the time when $P_i(t)$ is equal to 0.05 and the duration time, D_i, is defined as the time interval that $P_i(t)$ increases from 0.05 to 0.85. The shape of $P_i(t)$ is approximated by a function, $C_i(t)$, which is expressed by the two parameters, t_i and D_i, as follows:

$$C_i(t)=\begin{cases}(0.05/t_i)t & ;\ 0\le t<t_i \\ 1-\{2a^2(t-b)^2+2a(t-b)+1\}e^{-2a(t-b)} & ;\ t_i\le t\ ,\end{cases} \qquad (1)$$

where

$a=1.995/D_i$

$b=t_i-0.210D_i$.

The time history of a vertical ground motion generally has two peaks as mentioned previously. For this reason, the time history of a seismic ground motion is divided into two parts as shown in Fig.8. The preliminary part begins from the arrival of direct P wave. The boundary between the preliminary and the major parts is defined by the arrival time of direct S wave. The cumulative power curves of narrow band-pass filtered accelerograms for the two parts are separately modeled by the above three parameters, E_i, t_i, and D_i. The velocity response transfer function of a single degree of freedom oscillator with a damping ratio of 10 % is used as the narrow band-pass filter. Model parameters were determined for twelve central frequencies used by Izutani(1981). Twelve central frequencies of the narrow band-pass filter were chosen to be equally spaced in log-scale from log f_1 = -0.64 (f_1=0.23Hz) to log f_{12} = 1.12 (f_{12}=13.2Hz). Using the model parameters, synthetic accelerograms can be simulated as the summation of filtered shot-noise processes multiplied by a shape function.

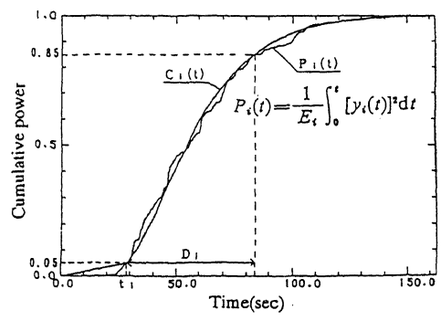

Fig.7 Modeling of cumulative power curve.

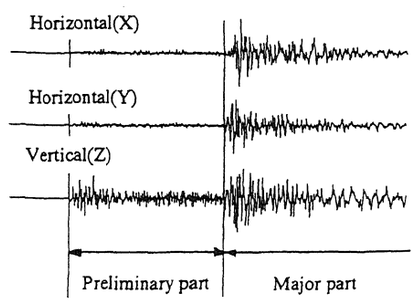

Fig.8 Division of seismic ground motion into preliminary and major parts.

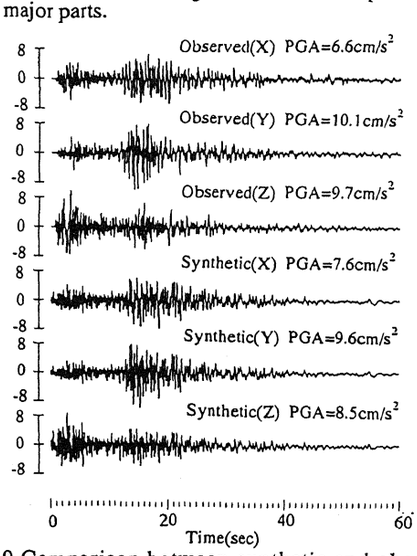

Fig.9 Comparison between synthetic and observed accelerograms.

The applicability of this simulation method is testified: Figure 9 shows the comparison between synthetic and observed accelerograms. The synthetic accelerograms were simulated by the proposed method using the model parameters obtained from the observed accelerograms.

The peak accelerations and the shape of the envelope are reproduced well by the simulation. The proposed simulation method for obtaining both horizontal and vertical synthetic accelerograms is proved to be applicable.

The relationships of the above model parameters between vertical and horizontal motions at the design base layer were examined using the observed strong ground motions at M. The location of the site is shown in Fig.1. The subsurface layer is composed of mudstone of the Miura group having a S wave velocity of about 700 m/s. The soil condition of the site is considered to be appropriate for examining the relationships at the design base layer. The model parameters were determined for the records of thirty-eight earthquakes with focal depths less than 100 km from 1982 through 1987. The magnitude-distance distribution of these earthquakes is shown in Fig.10. The histogram of the ratios of the vertical to the horizontal peak accelerations is shown in Fig.11. The mean ratio is 0.65 and most of the data are distributed in the range from 0.5 to 1.0. The ratio is relatively high if compared with those previously reported (for example, Omote and Narahashi(1978)). The ratios tend to become larger at the design base layer than those at the ground surface because the soil amplification nature differs between vertical and horizontal motions. This tendency is clearly shown in Fig.12. The ratios at the ground were obtained from the records of five stations described in Section 2. The records of the site F are excluded because no subsurface soil deposits exist. The outcropped free surface motions at the design base layer were estimated by 1-D wave propagation theory. P and S wave propagation theories are applied to vertical and horizontal motions respectively. The mean ratio at the design base layer is larger than that at the ground and is nearly equal to the mean ratio at M. This fact supports that the ground motion records at M are appropriate for examining the relationships at the design base layer.

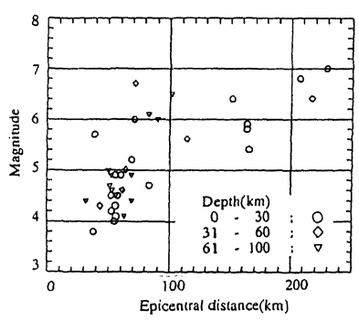

Fig.10 Magnitude-distance distribution of earthquaks used in the analysis.

Using the data obtained at M, the characteristics of waveform were examined in both frequency and time domains. Figure 13 shows the total power spectra of the preliminary and major parts for three earthquakes. The total power of vertical motion is higher than that of horizontal motion for the preliminary part, whereas the total power of horizontal motion is higher than that of vertical motion for the major part. The spectral shapes of vertical and horizontal motions for each part are almost similar. On the other hand the spectral shapes of the preliminary and major parts are very different. The spectra for the preliminary part have higher predominant frequencies than those for the major part. These natures are common for all earthquakes examined.

The mean relationships of the model parameters between vertical and horizontal motions were determined. The total power ratios and the differences of starting time and duration as a function of frequency are shown in Fig.14. Solid line denotes the mean and two broken lines denote the mean $\pm$ one standard deviation. Although the total power ratios for the major part tend to slightly increase with frequency higher than about 1 Hz, the dependence of the ratio on the frequency is not remarkable. This corresponds that the spectral shapes of vertical and horizontal motions for each part are similar. The starting time and duration of vertical motions are slightly smaller than those of horizontal motions for the preliminary part. This indicates that the power of vertical motions concentrate in the former part than that of horizontal. The vertical motions have a little longer duration than the horizontal motions for the major part.

Using the mean relationships of the model parameters in Fig.14, a vertical motion can be simulated from a horizontal motion given at the design base layer. If the deviations from the mean relationships correlate with magnitude, focal depth and epicentral distance, more accurate relationships between vertical and horizontal motions can be obtained; however, we could not find any significant correlation. The deviations from the mean relations may be controlled by the complex rupture process of an earthquake fault which can not be represented by simple parameters like magnitude.

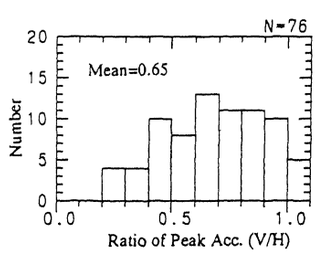

Fig.11 Histogram of the ratios of vertical to horizontal peak accelerations at M.

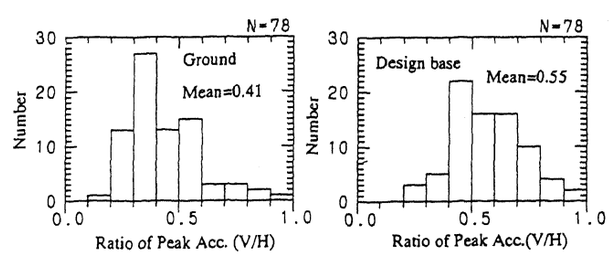

Fig.12 Histogram of the ratios of vertical to horizontal peak accelerations at the ground (left) and the design base (right) for the sites A to E.

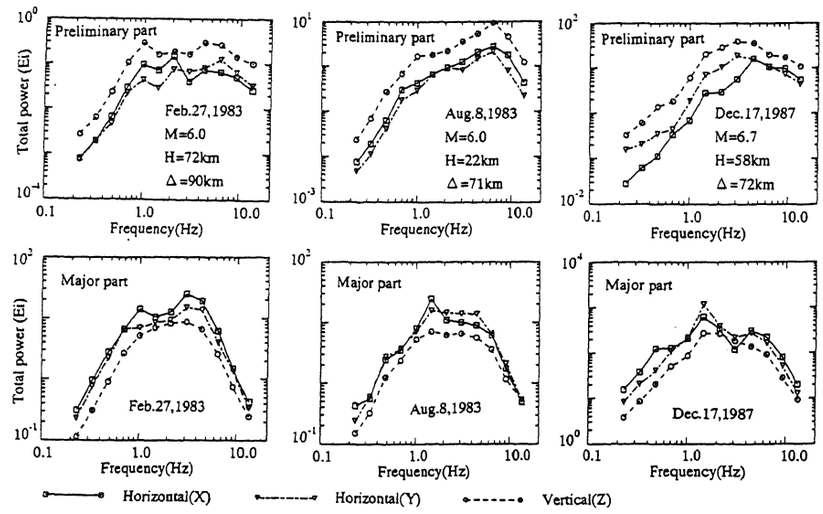

Fig.13 Total power spectra for three earthquakes.

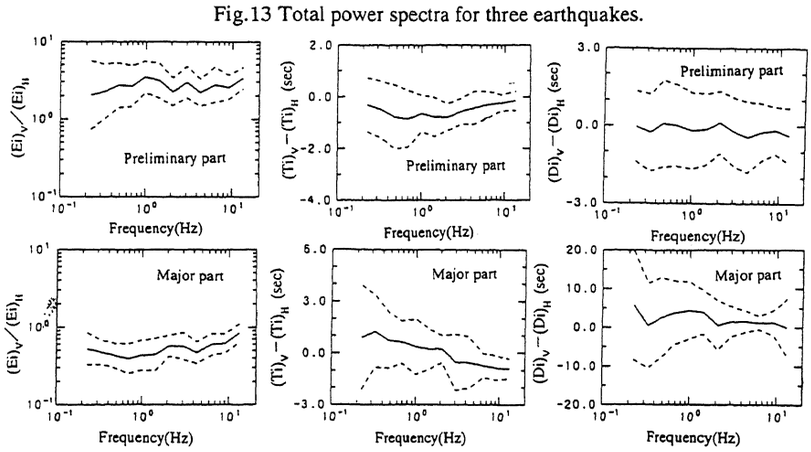

Fig.14 The ratio of total power spectra, the difference of starting times, and the difference of durations between vertical and horizontal motions. Suffixes of V and H denote vertical and horizontal motions respectively.

4 CONCLUSIONS

The applicability of P wave propagation theory to the vertical motion response analysis of soil to a vertical input motion was examined using strong motion accelerograms obtained by seismic vertical arrays. The results indicate that the main characteristics of the vertical soil response for both the P and S wave portions can be simulated by 1-D P wave propagation theory.

For examining the relationships between vertical and horizontal motions at the design base layer, a simulation method for obtaining both vertical and horizontal synthetic accelerograms was proposed. The mean relationships of the model parameters used in the simulation between vertical and horizontal motions were determined for a site with a subsurface S wave velocity of about 700 m/s. Using the mean relationships, it is possible to simulate a vertical motion from a horizontal motion given at the design base layer.

The effects of vertical motion can be taken into account in the soil response analysis by the above results.

REFERENCES

Izutani, Y. 1981. A statistical model for prediction of quasi-realistic strong ground motion, *J.Phys.Earth* 29:537-557.

Omote, S. and H.Narahashi 1978. A study on amplitude of vertical component in the strong earthquake motions, *Proc.5th Japan Earthq. Eng. Symp.* :1097-1104. (in Japanese with English abstract)